Free Radical Biology and Medicine 72 (2014) 257–266

Contents lists available at ScienceDirect

Free Radical Biology and Medicine

journal homepage: www.elsevier.com/locate/freeradbiomed

Original Contribution

Mg^{2+}- and ATP-dependent inhibition of transient receptor potential melastatin 7 by oxidative stress

Hana Inoue [a,*], Takashi Murayama [b], Michiko Tashiro [a], Takashi Sakurai [b], Masato Konishi [a]

[a] Department of Physiology, Tokyo Medical University, 160-8402 Tokyo, Japan
[b] Cellular and Molecular Pharmacology, Juntendo University Graduate School of Medicine, Tokyo, Japan

ARTICLE INFO

Article history:
Received 6 February 2014
Received in revised form
9 April 2014
Accepted 10 April 2014
Available online 18 April 2014

Keywords:
TRPM7
Oxidative stress
Reactive oxygen species
Free radicals

ABSTRACT

Transient receptor potential melastatin 7 (TRPM7) is a Ca^{2+}- and Mg^{2+}-permeable nonselective cation channel that contains a unique carboxyl-terminal serine/threonine protein kinase domain. It has been reported that reactive oxygen species associated with hypoxia or ischemia activate TRPM7 current and then induce Ca^{2+} overload resulting in neuronal cell death in the brain. In this study, we aimed to investigate the molecular mechanisms of TRPM7 regulation by hydrogen peroxide (H_2O_2) using murine TRPM7 expressed in HEK293 cells. Using the whole-cell patch-clamp technique, it was revealed that the TRPM7 current was inhibited, not activated, by the application of H_2O_2 to the extracellular solution. This inhibition was not reversed after washout or treatment with dithiothreitol, suggesting irreversible oxidation of TRPM7 or its regulatory factors by H_2O_2 under whole-cell recording. Application of an electrophile, *N*-methylmaleimide (NMM), which covalently modifies cysteine residues in proteins, also inhibited TRPM7 current irreversibly. The effects of H_2O_2 and NMM were dependent on free $[Mg^{2+}]_i$; the inhibition was stronger when cells were perfused with higher free $[Mg^{2+}]_i$ solutions via pipette. In addition, TRPM7 current was not inhibited by H_2O_2 when millimolar ATP was included in the intracellular solution, even in the presence of substantial free $[Mg^{2+}]_i$, which is sufficient for TRPM7 inhibition by H_2O_2 in the absence of ATP. Moreover, a kinase-deficient mutant of TRPM7 (K1645R) was similarly inhibited by H_2O_2 just like the wild-type TRPM7 in a $[Mg^{2+}]_i$- and $[ATP]_i$-dependent manner, indicating no involvement of the kinase activity of TRPM7. Thus, these data suggest that oxidative stress inhibits TRPM7 current under pathological conditions that accompany intracellular ATP depletion and free $[Mg^{2+}]_i$ elevation.

Reactive oxygen species (ROS) are implicated in various pathophysiological and physiological functions [1–5]. Several transient receptor potential (TRP) channels, including TRPM7, have been reported to be redox sensors that are activated by ROS and permeable to Ca^{2+} to induce cellular responses [6,7]. TRPM2 was the first reported ROS sensor among the TRP channels; the molecular mechanisms of redox sensing of TRPM2 have been vigorously investigated [8–11]. ROS stimulation generates nicotinamide adenosine dinucleotide, which is converted to ADP ribose (ADPR). The binding of ADPR to the NUDT9-H domain, located at the carboxyl terminus of TRPM2, activates the channel and thereby induces Ca^{2+} influx followed by cellular responses, such as cell death or inflammation. In contrast to the widely reported TRPM2, the mechanism of TRPM7 regulation by ROS has not been investigated to date. Aarts and colleagues [12] first reported that TRPM7 current is activated by ROS generated under anoxic conditions and induces neuronal cell death by Ca^{2+} overload. Subsequently, the downregulation of TRPM7 in hippocampal neurons has been reported to prevent delayed neuronal death after ischemia *in vivo* [13]. Thus TRPM7 plays a key role during oxidative stress, but the mechanism for the regulation by ROS remains unclear. In this study, we aimed to investigate the molecular mechanisms for the regulation of murine TRPM7 by ROS using heterologous expression systems in HEK293 cells. Unexpectedly, H_2O_2 did not activate, but rather inhibited, TRPM7 current under our conditions. The inhibition of TRPM7 current by H_2O_2 was dependent on intracellular concentrations of free Mg^{2+} ($[Mg^{2+}]_i$) and total ATP ($[ATP]_i$). When a kinase-deficient TRPM7 mutant was used, it was revealed that the kinase activity of TRPM7 was not involved in redox sensing. Our findings indicate that the activity of TRPM7 is inhibited by ROS in the presence of high $[Mg^{2+}]_i$ and low $[ATP]_i$, which may occur during prolonged ischemia. When $[ATP]_i$ is normal (~5 mM), on the other hand, TRPM7 activity is probably maintained even in the presence of ROS.

Portions of this work have appeared previously in abstract form [14].

* Corresponding author. Fax: +81 3 5379 0658.
E-mail address: hana@tokyo-med.ac.jp (H. Inoue).

http://dx.doi.org/10.1016/j.freeradbiomed.2014.04.015

Materials and methods

Cloning and generation of cell lines stably overexpressing TRPM7 and mutants

The full-length coding sequence of mouse TRPM7 (NM_001164325) was amplified by PCR using cDNA of mouse adipocytes as the template with the primers 5′-CC*ACGCGT*GCCACCATGTCCCAGAAATCCTGGATAG-3′ (MluI site is in italic) and 5′-CC*CTCGAG*CTATAACATCAGACGAACAG-3′ (XhoI site is in italic) and cloned into pcDNA5/FRT/TO (Invitrogen, Carlsbad, CA, USA), a tetracycline-inducible expression vector, using the MluI and XhoI sites. Single amino acid substitution mutants (K1645R and M1596A) were generated by site-directed mutagenesis using the QuikChange site-directed mutagenesis kit (Agilent Technologies, La Jolla, CA, USA) following the manufacturer's instructions. The predicted DNA sequences of all constructs were verified by sequencing. Stable inducible HEK293 cell lines expressing TRPM7 and its mutants were generated by cotransfection of the wild-type or mutant pcDNA5/FRT/TO vector with the pOG44 vector encoding Flp recombinase into Flp-In T-Rex HEK293 cells (Invitrogen), as previously described [15].

Cell culture

HEK293 TRPM7-wt, -K1645R, and -M1596A cells were maintained in Dulbecco's modified Eagle's medium supplemented with 10% fetal bovine serum, 2 mM glutamine, 100 μM hygromycin, 15 μM blasticidin, and penicillin–streptomycin (Invitrogen). To induce protein expression, doxycycline (1 μg/ml) was added to the culture medium the day before experiments. Experiments were performed 15–24 h postinduction.

Immunoblotting

Stable HEK293 cells were plated into 100-mm culture dishes and protein expression was induced by doxycycline (1 μg/ml) for 24 h. The cells were harvested, rinsed twice with phosphate-buffered saline, and resuspended in a homogenization buffer (0.3 M sucrose and 20 mM Tris–HCl, pH 7.4, and a protease inhibitor mixture). The cells were disrupted by N_2 cavitation after equilibration in N_2 for 15 min at 1000 psi. The microsomes were obtained by differential centrifugation (1000–100,000 *g*) and resuspended in the above buffer. These samples were mixed with Laemmli buffer and then subjected to SDS–PAGE (3–15%). The separated proteins were electrically transferred onto a polyvinylidene difluoride membrane. The membrane was incubated with goat anti-TRPM7 antibody (ab729; Abcam Biochemicals, Bristol, UK), followed by peroxidase-conjugated anti-goat IgG antibody (KPL, Gaithersburg, MD, USA). The positive bands were visualized using the enhanced chemiluminescence system.

Patch-clamp recordings

Stable HEK293 cells were plated on glass coverslips coated with Matrigel (BD Biosciences, Bedford, MA, USA). All recordings were conducted at room temperature (23–25 °C). A salt bridge containing 3 M KCl in 1.5% agarose was used to connect a reference Ag–AgCl electrode to minimize redox artifacts [16]. The patch electrodes were prepared from borosilicate glass capillaries and had a resistance of 1.5–2.3 MΩ when filled with a pipette solution (see below). Series resistance (< 3 MΩ) was compensated for (80%) to minimize voltage errors. Currents were recorded using an Axopatch 200B amplifier (Molecular Devices, Union City, CA, USA) coupled to a DigiData 1321A A/D and D/A converter (Molecular Devices). Current signals were filtered at 1 kHz using a four-pole Bessel filter and were digitized at 5 kHz. pClamp 10.2 software was used for the command pulse protocol, data acquisition, and analysis. The time courses of current were monitored by repetitively applying (every 10 s) a ramp pulse from −100 to +100 mV (1-s duration) from a holding potential of 0 mV. The control bath solution consisted of (in mM): 135 NaCl, 5 KCl, 1 $MgCl_2$, 1 $CaCl_2$, 1.2 NaH_2PO_4, 10 Hepes, 2 glucose, and 27 mannitol (pH 7.4 adjusted with NaOH, 315 mOsm/kg H_2O). The divalent-free bath solution (DVF) was made by omitting $MgCl_2$ and $CaCl_2$ and adding 0.5 mM EDTA and 0.2 mM EGTA. The intracellular (pipette) solutions were as follows (in mM): 25 CsCl, 110 CsOH, 110 glutamate, 0.2 EGTA, 10 EDTA, and 5 Hepes (pH 7.3 adjusted with CsOH, 290 mOsm/kg H_2O). $MgSO_4$ was added to vary the free Mg^{2+} concentrations ($[Mg^{2+}]$). For the intracellular solution containing $[Mg^{2+}]$ higher than 42.6 μM, EDTA was replaced with *N*-(2-Hydroxyethyl)ethylenediamine-*N,N′,N′*-triacetic acid (HEDTA). The ATP-containing intracellular solutions were as follows (in mM): 25 CsCl, 120 CsOH, 120 glutamate, 0.5 or 5 Na_2ATP, 0.1 NaGTP, and 5 Hepes. $MgCl_2$ was added to vary the $[Mg^{2+}]$. $[Mg^{2+}]$ was calculated by the Maxchelator software (http://maxchelator.stanford.edu/webmaxc/webmaxcS.htm). When adenosine 5′-(β,γ-imido)triphosphate (AMP-PNP) was included in place of ATP, $[Mg^{2+}]$ was estimated by using the dissociation constants reported by Pettit and Siddiqui [17]. The osmolarity of the intracellular solutions, ranging from 290 to 300 mOsm/kg H_2O, was measured using a freezing point depression osmometer (Osmomat 030, Gonotec, Berlin, Germany). H_2O_2 or *N*-methylmaleimide (NMM) was applied to the extracellular solution for 4 min, and the current amplitudes were analyzed at the end of the application. The current amplitudes just before the application of H_2O_2 or NMM were considered to represent the control.

Statistical analysis and data fitting

Data are given as means ± SEM of observations. Comparisons of two experimental groups were made using Student's *t* test, whereas multiple comparisons were made using ANOVA followed by the Bonferroni test. Data were considered to be significant at $P < 0.05$.

For analysis of concentration-dependent inhibition, data were fitted with a monophasic (Figs. 1D and 3C) or biphasic (Fig. 3D) concentration–response curve provided by the Origin software fitting subroutine (OriginLab, Northampton, MA, USA) as previously described [18]. The formula for monophasic concentration–response curves is

$$y = \text{Bottom} + [(\text{Top} - \text{Bottom})/(1 + 10^{(\log IC50 - x)\text{slope}})],$$

where Bottom and Top are the plateaus at the left and right ends of the curve. IC_{50} is the concentration that gives a half-maximal inhibitory effect. Slope is the unitless slope factor with a lower bound set to −10.

The formula for biphasic concentration–response curves with two IC_{50}'s, $IC_{50(1)}$ and $IC_{50(2)}$, is

$$y = \text{Bottom} + (\text{Top} - \text{Bottom})\,[p/(1 + 10^{(\log IC50(1) - x)\text{slope}1}) + (1-p)/(1 + 10^{(\log IC50(2) - x)\text{slope}2})],$$

where p is the fraction of high-affinity inhibition.

Results

TRPM7 inhibition by H_2O_2

To investigate the effect of H_2O_2 on TRPM7 current, we established a HEK293 cell line that expresses mouse TRPM7-wt by doxycycline treatment. Doxycycline-induced expression of TRPM7 was confirmed by Western blotting (cf Fig. 6A). Because it has been

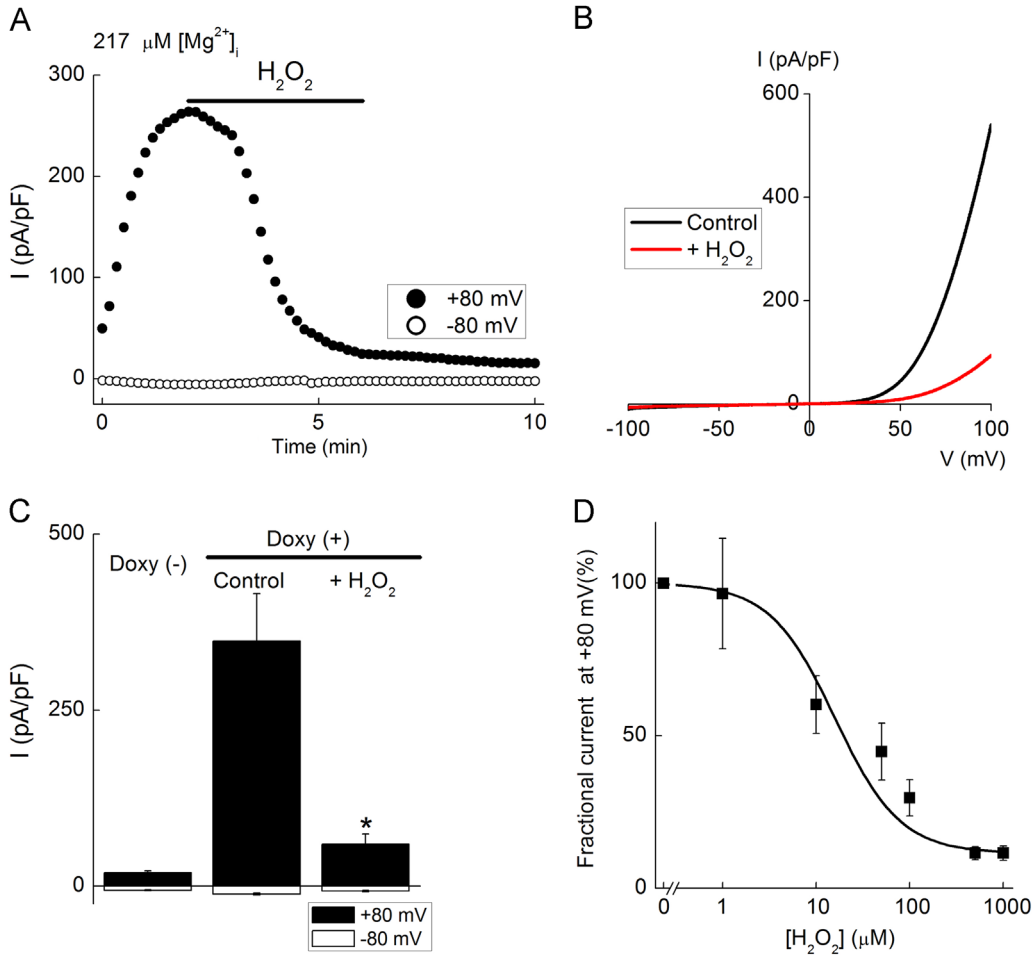

Fig. 1. TRPM7 inhibition by H_2O_2. (A) A representative trace showing the inhibitory effect of H_2O_2 (500 μM) on TRPM7-wt current in the presence of 217 μM $[Mg^{2+}]_i$. Under the whole-cell clamp mode, ramp command pulses from −100 to 100 mV (1-s duration) were applied every 10 s, and the current amplitude at +80 mV (closed circles) or −80 mV (open circles) was plotted against the recording time. (B) Representative *I–V* relationship of TRPM7-wt current recorded from the same cell shown in (A) before (black line) or 4 min after (red line) the application of H_2O_2 (500 μM). (C) Doxy treatment induced a substantial increase in the current density (at +80 mV, >10 times), which was inhibited by H_2O_2 (500 μM). Each bar represents the mean ± SEM (vertical bar) of seven to nine observations. *$P < 0.05$ vs control in Doxy (+) HEK293 cells. (D) H_2O_2 inhibited the current in a concentration-dependent manner with IC_{50} at 15.9 μM. Each symbol represents the mean current ± SEM (vertical bar) of the current amplitude at +80 mV after the application of H_2O_2 relative to that before application (4-6 observations).

reported that TRPM7 is inhibited by intracellular Mg^{2+} [18–20], we initially used a 217 μM Mg^{2+} intracellular solution, which enabled instantaneous recording of TRPM7 current after break-in. In doxycycline-treated [Doxy (+)] HEK293 cells, outwardly rectifying currents were gradually activated after break-in, probably due to relief from the inhibition by intracellular Mg^{2+} (Fig. 1A and B). In contrast, untreated [Doxy (−)] HEK293 cells exhibited a small outward current; the mean current density was <10% of Doxy (+) HEK293 cells (Fig. 1C).

Unexpectedly, application of 500 μM H_2O_2, which has been reported to induce an increase in $[Ca^{2+}]_i$ in HEK cells transfected with TRPM7 [21], did not activate, but rather inhibited, the currents (Fig. 1). The inhibition by H_2O_2 was irreversible after washout during recordings (~15 min) and it was concentration dependent with IC_{50} at 16 μM (Fig. 1D). Because spontaneous inactivation (rundown) of the current became prominent during whole-cell recordings over a period of ~15 min in the presence of 217 μM $[Mg^{2+}]_i$ (Supplementary Fig. 1A), it was difficult to determine whether washout of H_2O_2 for longer periods (>15 min) could reverse the inhibition of the TRPM7 current. However, even with a low concentration (10 μM) of H_2O_2, the inactivation of TRPM7 was not lowered after washout and after application of dithiothreitol (DTT) (Supplementary Fig. 1A). DTT applied immediately after 50 μM H_2O_2 treatment to minimize the effect of rundown had no effect on the current inactivation (Supplementary Fig. 1B). Thus, it was concluded that TRPM7 inhibition by H_2O_2 is irreversible at least under the present experimental conditions.

The fact that the current was induced by treatment with doxycycline, and it was inhibited by known inhibitors of TRPM7, 2-aminoethoxydiphenyl borate (200 μM) or NS8593 (30 μM), to 51.3 ± 4.8 ($n = 7$) or 10.3 ± 3.5% ($n = 5$) at +80 mV, respectively (data not shown), strongly suggested that the current was carried by TRPM7.

Voltage-independent inhibition of TRPM7 by H_2O_2

Extracellular divalent cations inhibit TRPM7 current in a voltage-dependent manner. Because the inward current is more sensitive to the blockade by divalent cations, the current–voltage (*I–V*) relationships exhibited strong outward rectification in the presence of divalent cations (Fig. 1B). Because the inward current was too small to investigate the effect of H_2O_2 in detail, divalent cations were eliminated from the extracellular solution to enhance inward current via TRPM7 (Fig. 2). Perfusion with DVF extracellular solution increased both the inward and the outward currents, resulting in quasi-linear *I–V* relationships in Doxy (+) TRPM7-wt

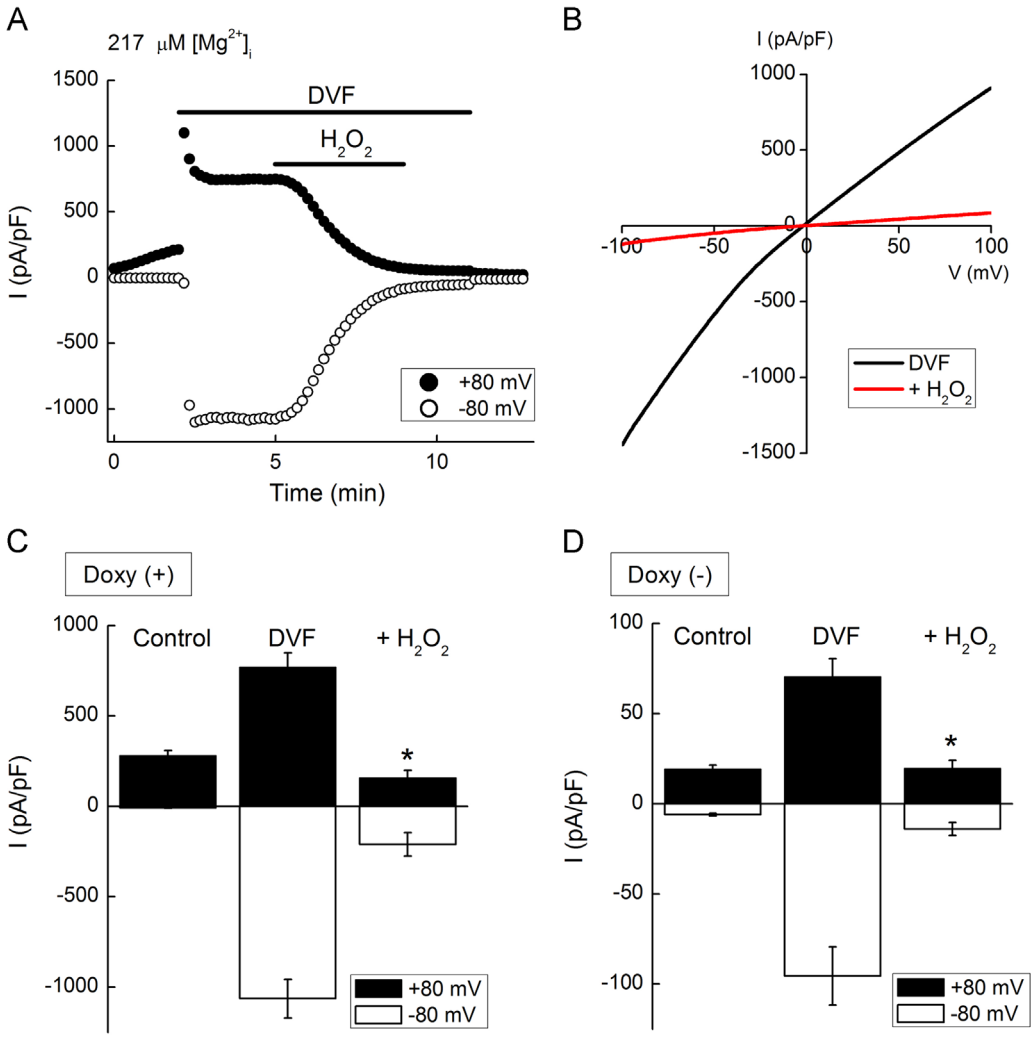

Fig. 2. TRPM7 inhibition by H_2O_2 was voltage independent. (A) A representative trace showing the voltage-independent inhibition of TRPM7 by H_2O_2 (500 μM). The current was activated by removal of extracellular divalent cations (DVF). Both inward and outward currents were inhibited by the application of H_2O_2 in the presence of 217 μM $[Mg^{2+}]_i$. (B) Representative *I–V* relationships of TRPM7-wt current recorded from the same cell shown in (A) in the absence (black line) or presence (red line) of H_2O_2 (500 μM) in the DVF solution. (C) Mean TRPM7-wt current densities from Doxy (+) HEK293 cells. Each bar represents the mean ± SEM (vertical bar) of 12 observations. $^*P < 0.05$ vs DVF. (D) Endogenous TRPM7-like current exhibited a similar sensitivity to H_2O_2 in Doxy (−) HEK293 cells. Each bar represents the mean current density ± SEM (vertical bar) of 6 observations. $^*P < 0.05$ vs DVF.

HEK293 cells (Fig. 2A and B). H_2O_2 (500 μM) inhibited both the inward and the outward currents to the same extent during DVF perfusion (Fig. 2B and C).

HEK293 cells have been reported to express native TRPM7 [19,22]. Consistently, Doxy (−) HEK293 cells exhibited a H_2O_2-sensitive current analogous to exogenously overexpressed TRPM7 under the DVF conditions, though the average current density was <10% of Doxy (+) HEK293 cells (Fig. 2D). Thus, voltage-independent inhibition of TRPM7 by H_2O_2 was similarly observed in native TRPM7, as well as in the overexpressed channels.

TRPM7 inhibition by H_2O_2 is dependent on $[Mg^{2+}]_i$

To investigate the effect of intracellular Mg^{2+} on the TRPM7 inhibition by H_2O_2, TRPM7 current was recorded in the absence or presence of H_2O_2 under various $[Mg^{2+}]_i$. As shown in Fig. 3A and B, there was no significant effect of H_2O_2 when intracellular Mg^{2+} was eliminated. When $[Mg^{2+}]_i$ was increased, a larger fraction of TRPM7 current was inhibited by H_2O_2 with IC_{50} at 25.1 μM $[Mg^{2+}]_i$ (Fig. 3C).

The TRPM7 current is inhibited by $[Mg^{2+}]_i$ in a concentration-dependent manner. Chokshi and colleagues [18] reported that the inhibition of TRPM7 by $[Mg^{2+}]_i$ is biphasic (i.e., two IC_{50} values), suggesting Mg^{2+} binding to the channel with two affinities. We therefore fitted the concentration–response relation for $[Mg^{2+}]_i$ with the biphasic function as employed in the previous study [18]. The data can be best fitted with $IC_{50(1)}$ of 6.5 μM and $IC_{50(2)}$ of 467.2 μM in the absence of H_2O_2 (Fig. 3D, black line); treatment with H_2O_2 (500 μM) shifted the curve leftward with IC_{50} values of 1.5 and 27.6 μM (Fig. 3D, red line). Thus, H_2O_2 seems to increase the sensitivity of TRPM7 to intracellular Mg^{2+}.

NMM inhibits TRPM7

H_2O_2 oxidizes proteins and alters their function. Cysteine residues of TRPM7 or its regulatory proteins are possible targets for oxidation by H_2O_2. Therefore we next investigated the effect of the synthetic cysteine-modification reagent, NMM, on TRPM7 current. As shown in Fig. 4, 100 μM NMM inhibited the TRPM7 current irreversibly. The inhibition was significant in the presence of intracellular Mg^{2+} (217 μM $[Mg^{2+}]_i$), whereas elimination of Mg^{2+} from the intracellular solution attenuated the inhibition by NMM (Fig. 4C). Taken together, these results suggest that H_2O_2 and NMM modify cysteine residues of TRPM7 or its regulator and

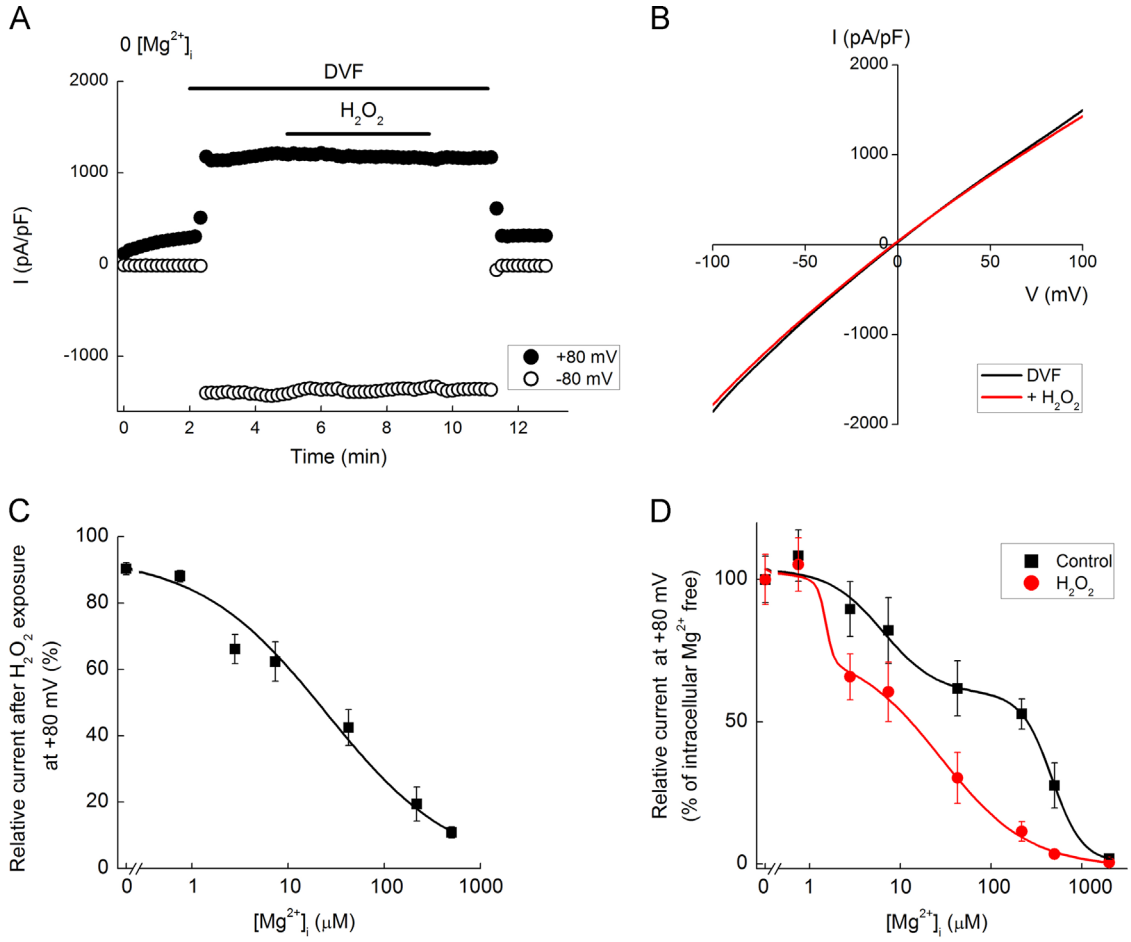

Fig. 3. TRPM7 inhibition by H_2O_2 was $[Mg^{2+}]_i$ dependent. (A) A representative trace showing no significant effect of H_2O_2 (500 μM) on TRPM7-wt current in the absence of intracellular Mg^{2+}. (B) Representative *I–V* relationships of TRPM7-wt current recorded from the same cell shown in (A) in the absence (black line) or presence (red line) of H_2O_2 (500 μM) in DVF solution. (C) H_2O_2 inhibited the current in a $[Mg^{2+}]_i$-dependent manner with IC_{50} at 25.1 μM. H_2O_2 was applied during perfusion with DVF solution. Each symbol represents the mean ± SEM (vertical bar) of the current density at +80 mV after the application of H_2O_2 relative to that before application (4–15 observations). (D) H_2O_2 increased the sensitivity of TRPM7-wt current to intracellular Mg^{2+}. H_2O_2 was applied during perfusion with DVF solution. TRPM7-wt current was inhibited by intracellular Mg^{2+} with $IC_{50(1)}$ value of 6.5 μM and $IC_{50(2)}$ value of 467.2 μM. After the treatment with H_2O_2 (500 μM), the IC_{50} values were changed to 1.5 and 27.6 μM, respectively. Each symbol represents the mean ± SEM (vertical bar) of the current density at +80 mV normalized to that at 0 $[Mg^{2+}]_i$ (4–15 observations).

thereby increase the TRPM7 sensitivity to intracellular Mg^{2+} and consequently inhibit the current.

TRPM7 inhibition by H_2O_2 is prevented by intracellular ATP

In addition to intracellular Mg^{2+}, ATP has also been reported to regulate TRPM7 activity [19,23,24]. To test the effect of ATP on TRPM7 inhibition by H_2O_2, TRPM7 current was recorded using intracellular solutions containing a total concentration of ATP of 5, 2, or 0.5 mM (Fig. 5). TRPM7 current was activated after break-in and further activated by extracellular perfusion with DVF in the presence of 5 mM $[ATP]_i$ and 199 μM $[Mg^{2+}]_i$. Application of H_2O_2 (500 μM), however, failed to significantly inhibit TRPM7 current (Fig. 5A and B). At lower intracellular [ATP], the inhibition by H_2O_2 became prominent (Fig. 5C). From these results, it is conceivable that in the presence of the normal level of $[ATP]_i$ (~5 mM), TRPM7 current is not inhibited by H_2O_2 even in the presence of substantial $[Mg^{2+}]_i$.

Activity of TRPM7 α-kinase is not related to the tolerance of TRPM7 currents to H_2O_2

TRPM7 harbors an α-kinase domain in its carboxyl terminus. Because tolerance to H_2O_2 was dependent on intracellular ATP (Fig. 5), we next investigated whether the kinase that requires ATP for its activity maintains the TRPM7 channel activity during H_2O_2 exposure. Another HEK cell line that expresses kinase-deficient TRPM7 (K1645R) was established, and the protein expression was confirmed by Western blotting (Fig. 6A). The effect of H_2O_2 on the mutant current was investigated in the presence of 217 μM $[Mg^{2+}]_i$ (Fig. 6B and C). Consistent with the previous study [25], kinase activity was not essential for the TRPM7 channel activity. As observed in TRPM7-wt, TRPM7-K1645R current was inhibited by H_2O_2 (500 μM) in a $[Mg^{2+}]_i$-dependent manner (Fig. 6D), and the presence of 5 mM $[ATP]_i$ prevented the current inhibition by H_2O_2 (cf Fig. 5C). Thus, even in the absence of kinase activity, ATP conferred the tolerance to H_2O_2 on TRPM7 channel activity (Fig. 6D).

Phosphatidylinositol 4,5-bisphosphate (PIP_2) supplementation does not affect the inhibition of TRPM7 by H_2O_2

Because the depletion of PIP_2 has been reported to inactivate the TRPM7 channel [26], we next examined the possibility that H_2O_2 inhibits TRPM7 via degradation of PIP_2. However, even when a high concentration of D-*myo*-phosphatidylinositol 4,5-bisphosphate (diC8-PIP_2) (20 or 50 μM) was added to the intracellular solution, TRPM7 was inhibited by H_2O_2 to a similar extent (Supplementary Fig. 2): 88.5 ± 2.1% (n = 4) in the absence of

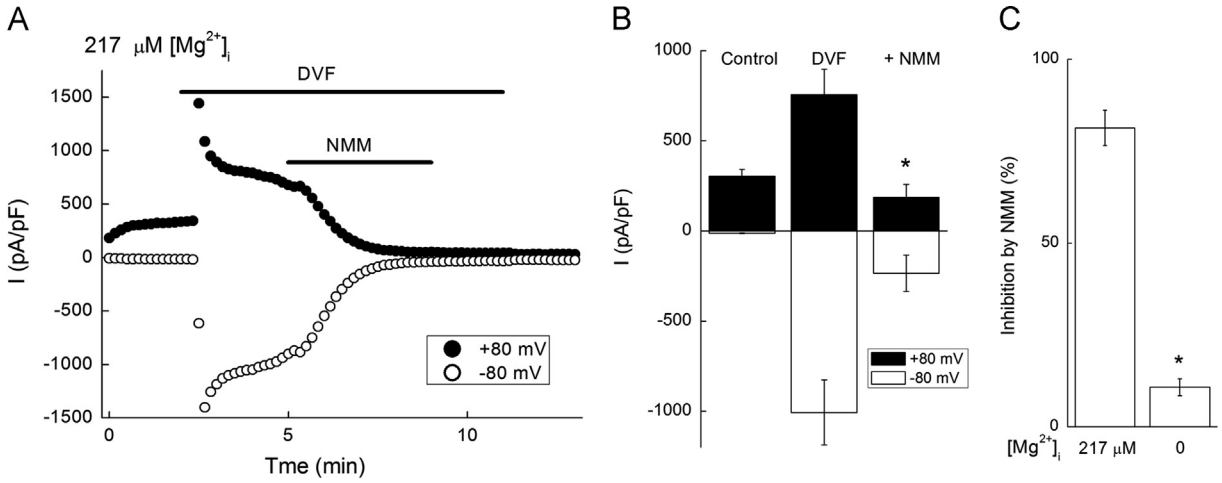

Fig. 4. The effect of NMM on TRPM7. (A) A representative trace showing the inhibitory effect of NMM (100 μM) on TRPM7-wt current in the presence of 217 μM $[Mg^{2+}]_i$. (B) Mean TRPM7-wt current density from Doxy (+) HEK293 cells. Each bar represents mean ± SEM (vertical bar) of 10 observations. *$P < 0.05$ vs DVF. (C) Elimination of Mg^{2+} significantly attenuated the inhibition of TRPM7-wt current by NMM. NMM was applied during perfusion with DVF solution. Each bar represents the mean ± SEM (vertical bar) of the fractional inhibition of the current at +80 mV by NMM (5–10 observations). *$P < 0.05$ vs 217 μM $[Mg^{2+}]_i$.

diC8-PIP_2 and 81.7 ± 1.8 ($n = 3$) or 83.9 ± 3.0% ($n = 5$) in the presence of 20 or 50 μM diC8-PIP_2 in the intracellular solution, respectively. These results indicate that PIP_2 is not involved in the ATP-dependent maintenance of TRPM7 activity during H_2O_2 exposure.

ATP hydrolysis is not necessary to prevent TRPM7 inhibition by H_2O_2

To test whether ATP hydrolysis is indispensable for the prevention of TRPM7 inhibition by H_2O_2, the nonhydrolyzable ATP analog AMP-PNP was included in place of ATP in the intracellular solution. In the presence of 5 mM $[AMP\text{-}PNP]_i$, H_2O_2 slightly inhibited TRPM7 current (Supplementary Fig. 3A), although the difference in the current density between before and 4 min after the application of H_2O_2 (500 μM) was not statistically significant ($P = 0.07$ or 0.09 at +80 or −80 mV, respectively; Supplementary Fig. 3B). The inhibition of TRPM7 current by H_2O_2 in the absence or presence of AMP-PNP was, on average, 81 or 47%, respectively (cf Fig. 2 and Supplementary Fig. 3B). AMP-PNP prevented TRPM7 inhibition by H_2O_2 (though less potent than ATP, cf Fig. 5), suggesting that hydrolysis of ATP is not necessary to maintain TRPM7 activity.

Molecular mechanisms underlying the inhibition by H_2O_2 differ between TRPM6 and TRPM7

TRPM6, the closest homolog of TRPM7, has been reported to be inhibited by H_2O_2 [27]. H_2O_2 oxidizes methionine 1755 of TRPM6 and thereby inactivates the channel. Mutation of M1755 to alanine makes TRPM6 resistant to the inactivation by H_2O_2 [27]. Therefore, M1596 of TRPM7, a residue corresponding to M1755 of TRPM6, was mutated to alanine to investigate whether this residue was involved in sensing oxidative stress and inactivating the channel as well. In contrast to TRPM6-M1755A, TRPM7-M1596A was inhibited by H_2O_2 (Fig. 6E). As with TRPM7-wt, the inhibition was dependent on $[Mg^{2+}]_i$, though an even lower concentration was sufficient to confer the inhibition (Fig. 6F).

Discussion

In this study, we demonstrated that TRPM7 was not activated, rather it was inhibited, by H_2O_2. Because both inward and outward currents were similarly inhibited by H_2O_2, the inhibition was voltage independent. Inhibition of TRPM7 current by H_2O_2 seems to result from increasing the sensitivity of the channel to intracellular Mg^{2+}. Furthermore, as intracellular ATP decreased, the inhibition was enhanced, suggesting that the intracellular energy level is an important factor for H_2O_2 inhibition of TRPM7. ATP maintains TRPM7 activity even in the presence of H_2O_2 by unknown mechanisms without the involvement of the α-kinase activity of TRPM7.

TRPM7 is inhibited by intracellular Mg^{2+} [19,20]. Recent elaborate studies by Chokshi and colleagues revealed that the TRPM7 channel is inhibited by internal Mg^{2+} in a biphasic manner, displaying both high- and low-affinity binding sites [18,28]. The present results also indicate two separate IC_{50} values for Mg^{2+} inhibition of high (~6.5 μM) and low (~467.2 μM) affinities (Fig. 3D). H_2O_2 treatment increased these affinities to ~1.5 and ~27.6 μM, respectively. To date, several amino acids in the TRPM7 C terminus have been reported to influence the sensitivity to intracellular Mg^{2+}. Consistent with the previous study by Schmitz and colleagues [25], we also observed that complete deletion of the C terminus after amino acid 1464 resulted in highly increased sensitivity to intracellular Mg^{2+} (data not shown). In the most recent paper by Hofmann and colleagues [29], the TRP domain in the TRPM7 C terminus was proposed to play a key role in the regulation by intracellular Mg^{2+}. Thus, the molecular structure of the TRPM7 C terminus is important for its sensitivity to Mg^{2+}. Oxidation of TRPM7 or its regulatory proteins by H_2O_2 might cause conformational changes in the channel molecule, possibly at sites proximal to the C terminus, that consequently lead to the increased affinities for Mg^{2+}.

Oxidative stress, including H_2O_2, induces oxidization of proteins at redox-sensitive amino acids, such as methionine and cysteine, and modulates their functions. In TRPM6, it has been reported that methionine (M1755) is oxidized by H_2O_2 and is reduced by methionine sulfoxide reductase B1 (MsrB1) [27]. Oxidation of M1755 results in the inactivation of TRPM6, whereas it is reversed by reduction by MsrB1 [27]. In contrast to TRPM6, an oxidation-resistant methionine mutant of TRPM7 (M1596A) was similarly inhibited by H_2O_2 just like TRPM7-wt (Fig. 6E and F). Thus, oxidation of this methionine residue is unlikely to play a role in the inhibition of TRPM7 by H_2O_2. Similar Mg^{2+}-dependent inhibition of TRPM7 by NMM suggests that cysteine residues are

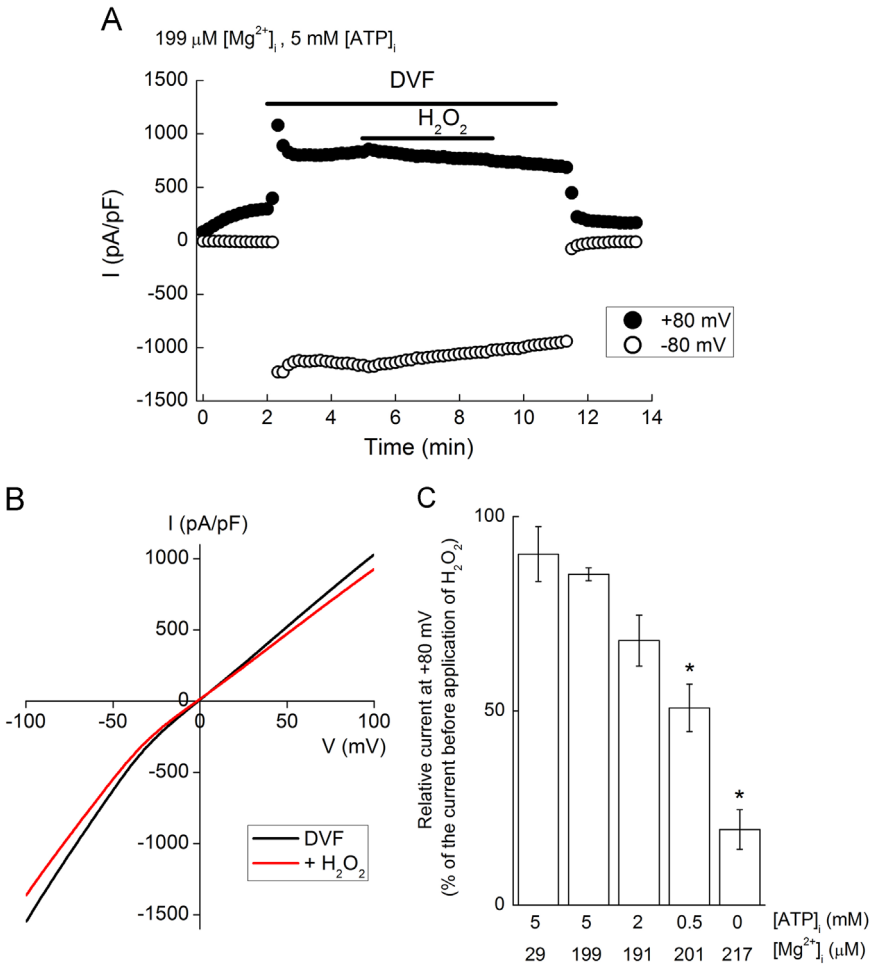

Fig. 5. The effect of intracellular ATP on TRPM7 inhibition by H_2O_2. H_2O_2 was applied during perfusion with DVF solution. (A) A representative trace showing no significant effect of H_2O_2 (500 μM) on TRPM7-wt current in the presence of 199 μM $[Mg^{2+}]_i$ and 5 mM $[ATP]_i$. (B) Representative *I–V* relationships of TRPM7-wt current recorded from the same cell shown in (A) in the absence (black line) or presence (red line) of H_2O_2 (500 μM) in DVF solution. (C) A decrease in $[ATP]_i$ increased the inhibitory effect of H_2O_2 on TRPM7-wt. The value for 0 $[ATP]_i$ and 217 μM $[Mg^{2+}]_i$ (the rightmost column) was taken from Fig. 3C. Each bar represents the mean ± SEM (vertical bar) of the current at +80 mV after the application of H_2O_2 relative to that before application (four to seven observations). *$P < 0.05$ vs 199 μM $[Mg^{2+}]_i$ and 5 mM $[ATP]_i$.

plausible targets for H_2O_2 oxidation to inhibit TRPM7 (Fig. 4C). There are 36 cysteine residues in a murine TRPM7 protein. Mutation of each cysteine residue may facilitate the identification of target residues of H_2O_2 oxidation that exert TRPM7 inactivation. Another maleimide, biotin maleimide, can be used to probe cysteine residues and, therefore, it might be a potential screening tool for the identification of the target cysteine residues if it can inhibit TRPM7 current as NMM does. However, extracellular application of biotin maleimide failed to inhibit TRPM7 current (Supplementary Fig. 4). It is conceivable that the target cysteine residues that must be oxidized for the inhibition of the current are not accessible by biotin maleimide (MW 451.54), a molecule larger than NMM (MW 111.10) or H_2O_2. Moreover, there is another possibility that yet unidentified proteins that regulate TRPM7 activity are the oxidation targets for H_2O_2. Oxidation of such regulatory proteins could influence the Mg^{2+} sensitivity of TRPM7 and thereby inactivate the channel.

Inhibition of TRPM7 by H_2O_2 was irreversible in this study. Even when a low concentration (10 μM) of H_2O_2 was applied, the TRPM7 current was not reversed after washout with DTT (Supplementary Fig. 1). The ineffectiveness of DTT suggests that target thiols are sulfinylated or sulfonylated. However, under the supposition that the target cysteine residues are localized intracellularly, it is still possible that the applied DTT from the extracellular side did not successfully access and reduce the oxidized thiols. Thus, it remains unclear if the oxidation that inactivates TRPM7 is reversible under physiological conditions, under which cells produce intracellular antioxidants, such as glutathione.

Interestingly, intracellular ATP supplementation prevented the inhibition of TRPM7 by H_2O_2 (Fig. 5). In the absence of ATP, 4-min treatment with H_2O_2 decreased the TRPM7 current to 19.5 ± 5.1% at +80 mV under 217 μM $[Mg^{2+}]_i$ conditions (Fig. 3C). In contrast, in the presence of 5 mM ATP, 85.1 ± 1.7% of the TRPM7 current remained after 4-min treatment with H_2O_2 under 199 μM $[Mg^{2+}]_i$ conditions (Fig. 5C). Of the supplemented 5 mM ATP in the intracellular solutions, it is estimated that 3.1 mM ATP forms Mg-ATP. Demeuse and colleagues [24] reported that intracellular Mg-ATP inhibits TRPM7 current with half-maximal inhibition at 3.33 mM in the presence of 210 μM $[Mg^{2+}]_i$. In the present study, however, Mg-ATP itself did not seem to inhibit TRPM7. Under ~200 μM $[Mg^{2+}]_i$ conditions, the mean current densities at +80 mV in the control extracellular solutions were not significantly different: 279.2 ± 30 pA/pF with 10 mM HEDTA and 287.1 ± 55.7 pA/pF with 5 mM ATP as a Mg^{2+} buffer. This result is consistent with a previous study by Kozak and Cahalan [30] showing that Mg-ATP acts only as a Mg^{2+} source, from which Mg^{2+} is released to inhibit TRPM7 channels. Thus, without affecting TRPM7 activity by itself, it remains unclear how ATP (or Mg-ATP) prevents the inhibition of TRPM7 current by H_2O_2. ATP is necessary for α-kinase at the TRPM7 C terminus to phosphorylate

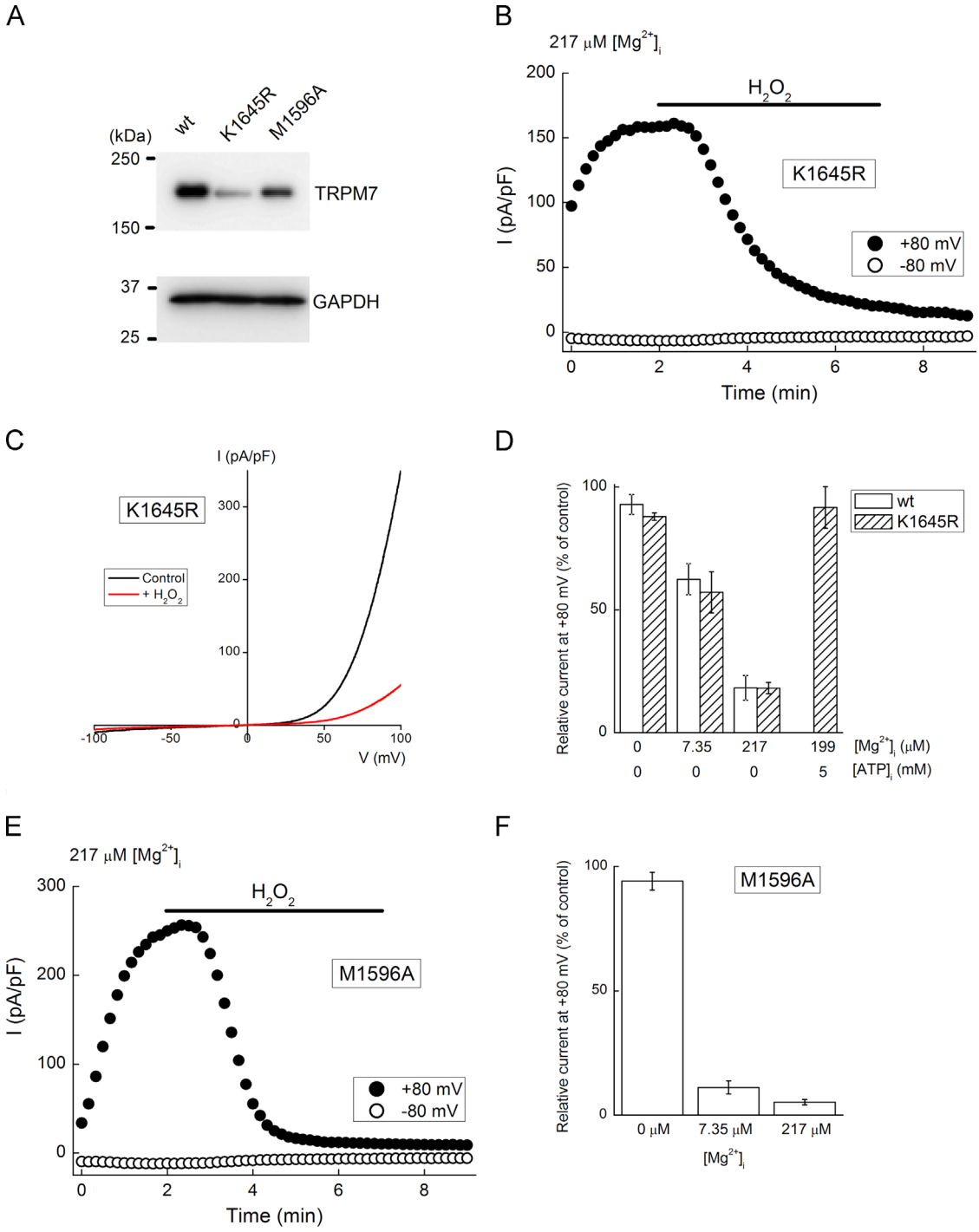

Fig. 6. The effect of H_2O_2 on TRPM7 mutants. (A) Doxy-induced protein expression of TRPM7 mutants, K1645R and M1596A, was confirmed by Western blot analysis. (B) A representative trace showing the inhibitory effect of H_2O_2 (500 μM) on TRPM7-K1645R current in the presence of 217 μM $[Mg^{2+}]_i$. (C) Representative *I–V* relationship of TRPM7-K1645R current recorded from the same cell shown in (B) before (black line) or 4 min after (red line) the application of H_2O_2 (500 μM). (D) Inhibition of TRPM7-K1645R by H_2O_2 was dependent on $[Mg^{2+}]_i$ and $[ATP]_i$. H_2O_2 was applied during the perfusion with control solution. Each bar represents the mean ± SEM (vertical bar) of the current density at +80 mV after the application of H_2O_2 relative to that before application (4–14 observations). (E) Representative traces showing the inhibitory effect of H_2O_2 (500 μM) on TRPM7-M1596A current in the presence of 217 μM $[Mg^{2+}]_i$. (F) Inhibition of TRPM7-M1596A by H_2O_2 was similar to TRPM7-wt. H_2O_2 was applied during the perfusion with control solution. Each bar represents the mean ± SEM (vertical bar) of the current at +80 mV after the application of H_2O_2 relative to that before application (5–8 observations).

its targets by donating a terminal phosphate. Therefore, it was suggested that ATP supplementation prevented the inhibition by keeping the phosphorylation activity of TRPM7 α-kinase. However, by using a kinase-deficient TRPM7 mutant (K1645R), it was revealed that ATP confers the tolerance to H_2O_2 without TRPM7 α-kinase activity (Fig. 6D).

PIP_2 has been reported to be a regulator for TRPM7 activity [26,31,32]. Because PIP_2 synthesis is catalyzed by phosphatidylinositol-4-phosphate 5 kinase (PIP5K), which also requires ATP, PIP5K activity sustained by ATP supplementation is probably involved in the tolerance to H_2O_2. Additionally, it has been reported that H_2O_2 decreases PIP_2 levels by downregulating PIP5K [33,34]. In conjunction

with these previous studies, it is tempting to hypothesize that PIP_2 plays a central role in the TRPM7 tolerance to H_2O_2, that is, H_2O_2 decreases PIP_2 levels by downregulating PIP5K and thereby inactivating TRPM7. However, intracellular supplementation of PIP_2 failed to prevent the inhibition of TRPM7 by H_2O_2 (Supplementary Fig. 2). Thus, the involvement of PIP_2 in the regulation of TRPM7 by ROS is unlikely.

The above two denied hypotheses (the involvement of TRPM7 α-kinase or PIP_2) both require ATP hydrolysis. Consistently, as shown in Supplementary Fig. 3, it was revealed that a nonhydrolyzable ATP analog, AMP-PNP, also prevented TRPM7 inhibition by H_2O_2, though the effect was less potent than that of ATP. It has been reported that AMP-PNP acts like ATP, but with lower affinities, on several ion channels and membrane proteins [35–37]. It is thus plausible that ATP binding, rather than its hydrolysis, plays a crucial role in the maintenance of TRPM7 activity during H_2O_2 exposure. The partial effect of AMP-PNP on TRPM7 activity observed in this study might be due to such a lower affinity binding to ATP acting sites. Further study is necessary to determine the precise mechanisms for ATP-induced tolerance of TRPM7 to oxidative stress.

The effects of free Mg^{2+} and ATP on TRPM7 under oxidative stress might be of physiological relevance. Because ATP binds Mg^{2+} with a high affinity (K_d ~100 μM), most intracellular ATP forms Mg-ATP. During ischemia or hypoxia, hydrolysis of Mg-ATP causes the rise in $[Mg^{2+}]_i$. In concert with low $[ATP]_i$ and high $[Mg^{2+}]_i$, ROS, which are also produced under these conditions, should strongly inhibit TRPM7.

In contrast to this study, Aarts and colleagues [12] reported that in TRPM7-overexpressing HEK293 cells, which are quite similar to our cell line, the application of 1 mM H_2O_2 slightly inhibited the outward current but markedly enhanced the inward current. The discrepancy between their study and our present results in the effect of H_2O_2 on TRPM7 might be explained by the differences in recording conditions. In their study, the intracellular solution contained 5 mM ATP and 1 mM $MgCl_2$ (calculated $[Mg^{2+}] < 30$ μM) and 1 mM H_2O_2 was applied for over 30 min. In our study, under similar intracellular conditions, 500 μM or 1 mM H_2O_2 slightly but not significantly inhibited both inward and outward TRPM7 currents during a 4-min application (Fig. 5C and Supplementary Fig. 5). Because the inhibitory effect of H_2O_2 on TRPM7 occurred immediately after application (Figs. 1 and 2), we did not examine the effect of long-term exposure to H_2O_2 on TRPM7 current in the presence of 5 mM $[ATP]_i$. A recent study by Desai and colleagues [38] demonstrated that apoptotic stimuli cleaved TRPM7 at D1510 by caspase 3, as well as by caspase 8, and consequently increased TRPM7 currents. H_2O_2 has been reported to induce activation of caspases [5,39]. It might be possible that such mechanisms are involved in the late enhancement of TRPM7 current observed in the previous study by Aarts and colleagues [12]. Further investigation is necessary to clarify the time course of the effect of oxidative stress on TRPM7.

What is the physiological significance of TRPM7 inhibition by oxidative stress? TRPM7 permeates divalent cations, including Ca^{2+} and Mg^{2+}, as well as Zn^{2+}; therefore inhibition of TRPM7 prevents the influx of these cations. In neurons, in addition to Ca^{2+} overload mediated by TRPM7-induced cell death [12], Zn^{2+} influx via TRPM7 may induce neurotoxicity [40]. TRPM7 also mediates Mg^{2+} influx during cell stress, and intracellular Mg^{2+} has been reported to promote intracellular ROS production [41–43]. During ischemia and hypoxia, $[ATP]_i$ decreases and $[Mg^{2+}]_i$ increases in severely affected cells owing to ATP degradation. In such cells, ROS inhibit TRPM7 to prevent further influx of Ca^{2+}, Zn^{2+}, and Mg^{2+} that may exacerbate cell damage. Thus, the mechanism of TRPM7 inhibition by ROS may work as an innate safety system to prevent progressive damage in cells whose metabolism is disturbed.

Acknowledgments

We thank S. Tai for secretarial assistance. This study was funded by a JSPS Grant-in-Aid for Young Scientists (B) (No. 22790220) and a JSPS Grant-in-Aid for Scientific Research (C) (No. 25460302), and it was supported by the Hiroshi and Aya Irisawa Memorial Promotion Award for Young Physiologists.

Appendix A. Supplementary material

Supplementary data associated with this article can be found in the online version at http://dx.doi.org/10.1016/j.freeradbiomed.2014.04.015.

References

[1] Evans, J. L.; Maddux, B. A.; Goldfine, I. D. The molecular basis for oxidative stress-induced insulin resistance. *Antioxid. Redox Signaling* **7:**1040–1052; 2005.
[2] Goldstein, B. J.; Mahadev, K.; Wu, X.; Zhu, L.; Motoshima, H. Role of insulin-induced reactive oxygen species in the insulin signaling pathway. *Antioxid. Redox Signaling* **7:**1021–1031; 2005.
[3] Kourie, J. I. Interaction of reactive oxygen species with ion transport mechanisms. *Am. J. Physiol.* **275:**C1–24; 1998.
[4] Ray, P. D.; Huang, B. W.; Tsuji, Y. Reactive oxygen species (ROS) homeostasis and redox regulation in cellular signaling. *Cell. Signalling* **24:**981–990; 2012.
[5] Kamata, H.; Hirata, H. Redox regulation of cellular signalling. *Cell. Signalling* **11:**1–14; 1999.
[6] Kozai, D.; Ogawa, N.; Mori, Y. Redox regulation of transient receptor potential channels. *Antioxid. Redox Signaling*, 2013. 10.1089/ars.2013.5616, online publication.
[7] Simon, F.; Varela, D.; Cabello-Verrugio, C. Oxidative stress-modulated TRPM ion channels in cell dysfunction and pathological conditions in humans. *Cell. Signalling* **25:**1614–1624; 2013.
[8] Wehage, E.; Eisfeld, J.; Heiner, I.; Jungling, E.; Zitt, C.; Luckhoff, A. Activation of the cation channel long transient receptor potential channel 2 (LTRPC2) by hydrogen peroxide: a splice variant reveals a mode of activation independent of ADP-ribose. *J. Biol. Chem.* **277:**23150–23156; 2002.
[9] Hara, Y.; Wakamori, M.; Ishii, M.; Maeno, E.; Nishida, M.; Yoshida, T.; Yamada, H.; Shimizu, S.; Mori, E.; Kudoh, J.; Shimizu, N.; Kurose, H.; Okada, Y.; Imoto, K.; Mori, Y. LTRPC2 Ca^{2+}-permeable channel activated by changes in redox status confers susceptibility to cell death. *Mol. Cell* **9:**163–173; 2002.
[10] Toth, B.; Csanady, L. Identification of direct and indirect effectors of the transient receptor potential melastatin 2 (TRPM2) cation channel. *J. Biol. Chem.* **285:**30091–30102; 2010.
[11] Perraud, A. L.; Takanishi, C. L.; Shen, B.; Kang, S.; Smith, M. K.; Schmitz, C.; Knowles, H. M.; Ferraris, D.; Li, W.; Zhang, J.; Stoddard, B. L.; Scharenberg, A. M. Accumulation of free ADP-ribose from mitochondria mediates oxidative stress-induced gating of TRPM2 cation channels. *J. Biol. Chem.* **280:**6138–6148; 2005.
[12] Aarts, M.; Iihara, K.; Wei, W. L.; Xiong, Z. G.; Arundine, M.; Cerwinski, W.; MacDonald, J. F.; Tymianski, M. A key role for TRPM7 channels in anoxic neuronal death. *Cell* **115:**863–877; 2003.
[13] Sun, H. S.; Jackson, M. F.; Martin, L. J.; Jansen, K.; Teves, L.; Cui, H.; Kiyonaka, S.; Mori, Y.; Jones, M.; Forder, J. P.; Golde, T. E.; Orser, B. A.; Macdonald, J. F.; Tymianski, M. Suppression of hippocampal TRPM7 protein prevents delayed neuronal death in brain ischemia. *Nat. Neurosci.* **12:**1300–1307; 2009.
[14] Inoue, H.; Murayama, T.; Konishi, M. TRPM7 kinase activity is not necessary for oxidative stress-induced current inhibition. *J. Physiol. Sci.* **64:**S175; 2014.
[15] Murayama, T.; Kurebayashi, N.; Oba, T.; Oyamada, H.; Oguchi, K.; Sakurai, T.; Ogawa, Y. Role of amino-terminal half of the S4-S5 linker in type 1 ryanodine receptor (RyR1) channel gating. *J. Biol. Chem.* **286:**35571–35577; 2011.
[16] Berman, J. M.; Awayda, M. S. Redox artifacts in electrophysiological recordings. *Am. J. Physiol. Cell Physiol.* **304:**C604–C613; 2013.
[17] Pettit, L. D.; Siddiqui, K. F. The proton and metal complexes of adenyl-5′-yl imidodiphosphate. *Biochem. J.* **159:**169–171; 1976.
[18] Chokshi, R.; Matsushita, M.; Kozak, J. A. Detailed examination of Mg^{2+} and pH sensitivity of human TRPM7 channels. *Am. J. Physiol. Cell Physiol.* **302:**C1004–-C1011; 2012.
[19] Nadler, M. J.; Hermosura, M. C.; Inabe, K.; Perraud, A. L.; Zhu, Q.; Stokes, A. J.; Kurosaki, T.; Kinet, J. P.; Penner, R.; Scharenberg, A. M.; Fleig, A. LTRPC7 is a Mg.ATP-regulated divalent cation channel required for cell viability. *Nature* **411:**590–595; 2001.
[20] Prakriya, M.; Lewis, R. S. Separation and characterization of currents through store-operated CRAC channels and Mg^{2+}-inhibited cation (MIC) channels. *J. Gen. Physiol.* **119:**487–507; 2002.
[21] Yoshida, T.; Inoue, R.; Morii, T.; Takahashi, N.; Yamamoto, S.; Hara, Y.; Tominaga, M.; Shimizu, S.; Sato, Y.; Mori, Y. Nitric oxide activates TRP channels by cysteine S-nitrosylation. *Nat. Chem. Biol.* **2:**596–607; 2006.
[22] Zhang, Z.; Yu, H.; Huang, J.; Faouzi, M.; Schmitz, C.; Penner, R.; Fleig, A. The TRPM6 kinase domain determines the Mg ATP sensitivity of TRPM7/M6 heteromeric ion channels. *J. Biol. Chem.* **289:**5217–5227; 2014.

[23] Runnels, L. W.; Yue, L.; Clapham, D. E. TRP-PLIK, a bifunctional protein with kinase and ion channel activities. *Science* **291:**1043–1047; 2001.
[24] Demeuse, P.; Penner, R.; Fleig, A. TRPM7 channel is regulated by magnesium nucleotides via its kinase domain. *J. Gen. Physiol.* **127:**421–434; 2006.
[25] Schmitz, C.; Perraud, A. L.; Johnson, C. O.; Inabe, K.; Smith, M. K.; Penner, R.; Kurosaki, T.; Fleig, A.; Scharenberg, A. M. Regulation of vertebrate cellular Mg^{2+} homeostasis by TRPM7. *Cell* **114:**191–200; 2003.
[26] Runnels, L. W.; Yue, L.; Clapham, D. E. The TRPM7 channel is inactivated by PIP(2) hydrolysis. *Nat. Cell Biol.* **4:**329–336; 2002.
[27] Cao, G.; Lee, K. P.; van der Wijst, J.; de Graaf, M.; van der Kemp, A.; Bindels, R. J.; Hoenderop, J. G. Methionine sulfoxide reductase B1 (MsrB1) recovers TRPM6 channel activity during oxidative stress. *J. Biol. Chem.* **285:**26081–-26087; 2010.
[28] Chokshi, R.; Matsushita, M.; Kozak, J. A. Sensitivity of TRPM7 channels to Mg^{2+} characterized in cell-free patches of Jurkat T lymphocytes. *Am. J. Physiol. Cell Physiol.* **302:**C1642–C1651; 2012.
[29] Hofmann, T.; Schafer, S.; Linseisen, M.; Sytik, L.; Gudermann, T.; Chubanov, V. Activation of TRPM7 channels by small molecules under physiological conditions. *Pflugers Arch.*; 2014. 10.1007/s00424-014-1488-0, published on-line.
[30] Kozak, J. A.; Cahalan, M. D. MIC channels are inhibited by internal divalent cations but not ATP. *Biophys. J.* **84:**922–927; 2003.
[31] Gwanyanya, A.; Sipido, K. R.; Vereecke, J.; Mubagwa, K. ATP and PIP_2 dependence of the magnesium-inhibited, TRPM7-like cation channel in cardiac myocytes. *Am. J. Physiol. Cell Physiol.* **291:**C627–C635; 2006.
[32] Kozak, J. A.; Matsushita, M.; Nairn, A. C.; Cahalan, M. D. Charge screening by internal pH and polyvalent cations as a mechanism for activation, inhibition, and rundown of TRPM7/MIC channels. *J. Gen. Physiol.* **126:**499–514; 2005.
[33] Chen, M. Z.; Zhu, X.; Sun, H. Q.; Mao, Y. S.; Wei, Y.; Yamamoto, M.; Yin, H. L. Oxidative stress decreases phosphatidylinositol 4,5-bisphosphate levels by deactivating phosphatidylinositol-4-phosphate 5-kinase beta in a Syk-dependent manner. *J. Biol. Chem.* **284:**23743–23753; 2009.
[34] Mesaeli, N.; Tappia, P. S.; Suzuki, S.; Dhalla, N. S.; Panagia, V. Oxidants depress the synthesis of phosphatidylinositol 4,5-bisphosphate in heart sarcolemma. *Arch. Biochem. Biophys.* **382:**48–56; 2000.
[35] Paulais, M.; Teulon, J. A cation channel in the thick ascending limb of Henle's loop of the mouse kidney: inhibition by adenine nucleotides. *J. Physiol.* **413:**315–327; 1989.
[36] Aleksandrov, A. A.; Chang, X.; Aleksandrov, L.; Riordan, J. R. The non-hydrolytic pathway of cystic fibrosis transmembrane conductance regulator ion channel gating. *J. Physiol.* **528(Pt 2):**259–265; 2000.
[37] Yu, G. H.; Ward, P. A. Structural requirements for binding of adenosine-5′-O-(3-thiotriphosphate) (ATP gamma S) to human neutrophils. *Immunopharmacology* **20:**175–182; 1990.
[38] Desai, B. N.; Krapivinsky, G.; Navarro, B.; Krapivinsky, L.; Carter, B. C.; Febvay, S.; Delling, M.; Penumaka, A.; Ramsey, I. S.; Manasian, Y.; Clapham, D. E. Cleavage of TRPM7 releases the kinase domain from the ion channel and regulates its participation in Fas-induced apoptosis. *Dev. Cell* **22:**1149–1162; 2012.
[39] Ryter, S. W.; Kim, H. P.; Hoetzel, A.; Park, J. W.; Nakahira, K.; Wang, X.; Choi, A. M. Mechanisms of cell death in oxidative stress. *Antioxid. Redox Signaling* **9:**49–89; 2007.
[40] Inoue, K.; Branigan, D.; Xiong, Z. G. Zinc-induced neurotoxicity mediated by transient receptor potential melastatin 7 channels. *J. Biol. Chem.* **285:**7430–-7439; 2010.
[41] Su, L. T.; Chen, H. C.; Gonzalez-Pagan, O.; Overton, J. D.; Xie, J.; Yue, L.; Runnels, L. W. TRPM7 activates m-calpain by stress-dependent stimulation of p38 MAPK and c-Jun N-terminal kinase. *J. Mol. Biol.* **396:**858–869; 2010.
[42] Chen, H. C.; Su, L. T.; Gonzalez-Pagan, O.; Overton, J. D.; Runnels, L. W. A key role for Mg^{2+} in TRPM7's control of ROS levels during cell stress. *Biochem. J.* **445:**441–448; 2012.
[43] Tamura, M.; Kanno, M.; Kai, T. Destabilization of neutrophil NADPH oxidase by ATP and other trinucleotides and its prevention by Mg^{2+}. *Biochim. Biophys. Acta* **1510:**270–277; 2001.